Neuron
Article

Excitatory Interactions between Olfactory Processing Channels in the *Drosophila* Antennal Lobe

Shawn R. Olsen,[1,2] Vikas Bhandawat,[1,2] and Rachel I. Wilson[1,*]
[1] Department of Neurobiology, Harvard Medical School, 220 Longwood Avenue, Boston, MA 02115, USA
[2] These authors contributed equally to this work.
*Correspondence: rachel_wilson@hms.harvard.edu
DOI 10.1016/j.neuron.2007.03.010

SUMMARY

Each odorant receptor gene defines a unique type of olfactory receptor neuron (ORN) and a corresponding type of second-order neuron. Because each odor can activate multiple ORN types, information must ultimately be integrated across these processing channels to form a unified percept. Here, we show that, in *Drosophila*, integration begins at the level of second-order projection neurons (PNs). We genetically silence all the ORNs that normally express a particular odorant receptor and find that PNs postsynaptic to the silent glomerulus receive substantial lateral excitatory input from other glomeruli. Genetically confining odor-evoked ORN input to just one glomerulus reveals that most PNs postsynaptic to other glomeruli receive indirect excitatory input from the single ORN type that is active. Lateral connections between identified glomeruli vary in strength, and this pattern of connections is stereotyped across flies. Thus, a dense network of lateral connections distributes odor-evoked excitation between channels in the first brain region of the olfactory processing stream.

INTRODUCTION

All the olfactory receptor neurons (ORNs) that express the same odorant receptor gene respond similarly to odors, and all project to the same sphere of neuropil (glomerulus) in the brain (Buck, 1996). Furthermore, in most species, each second-order olfactory neuron receives direct synaptic input from only one glomerulus. Thus, each odorant receptor gene defines a unique parallel processing channel in the olfactory system.

There is good evidence for crosstalk between these glomerular channels very early in the olfactory system, as early as the level of second-order neurons. Anatomically, glomeruli are interconnected by a network of local interneurons. Functionally, synaptic connections have been demonstrated between interneurons and second-order principal neurons, both in the insect antennal lobe and in the mammalian olfactory bulb (Jahr and Nicoll, 1980; Ernst and Boeckh, 1983; Hoskins et al., 1986; Malun, 1991; Leitch and Laurent, 1996; MacLeod and Laurent, 1996; Stocker et al., 1997; Christensen et al., 1998; Isaacson and Strowbridge, 1998; Python and Stocker, 2002; Urban and Sakmann, 2002; Aungst et al., 2003; Hayar et al., 2004; Wilson et al., 2004; Wilson and Laurent, 2005). It seems likely that these lateral connections have a role in shaping the output of the olfactory bulb and the antennal lobe. However, none of these studies has directly assessed the net effect of glomerular crosstalk on second-order neurons during in vivo odor stimulation.

Understanding how the antennal lobe and olfactory bulb transform olfactory representations requires an in vivo characterization of interglomerular synaptic connections. Is the net effect of these lateral connections inhibitory or excitatory? How powerful are these connections compared to direct ORN inputs? How does the amount of lateral input to a second-order neuron vary across odor stimuli? What rules govern the pattern of synaptic connectivity between glomeruli? Is a single glomerulus only connected with glomeruli in its local vicinity? Is each glomerulus only connected to a few others, or is the pattern of connectivity more dense? Is there a correlation between glomerular connectivity and odor tuning? To what extent is the pattern of lateral connectivity stereotyped from one animal to the next?

The most direct way to characterize lateral input to a second-order olfactory neuron would be to silence its direct ORN inputs while preserving ORN input to another glomerulus or glomeruli. Any remaining odor responses in cells postsynaptic to a "silent" glomerulus should reflect purely lateral inputs. This type of experiment is currently not possible in vertebrates, so we have turned to the *Drosophila* antennal lobe. This structure shares the same basic architecture as the vertebrate olfactory bulb but presents several experimental advantages. First, the odorant receptor gene expressed by most *Drosophila* ORN types has already been identified and mapped onto spatially stereotyped glomeruli in the antennal lobe

(Couto et al., 2005; Fishilevich and Vosshall, 2005; Hallem and Carlson, 2006). Second, the circuitry of the *Drosophila* antennal lobe develops properly in the absence of normal olfactory activity, and ORNs target the correct glomerulus even when they do not express a functional receptor (Dobritsa et al., 2003; Berdnik et al., 2006). Finally there are only ~50 glomeruli in the *Drosophila* antennal lobe, as compared to ~1000 in the mouse olfactory bulb (Laissue et al., 1999). This makes it possible to record from second-order neurons (called projection neurons, or PNs) postsynaptic to an identified ORN input. Importantly, like olfactory bulb mitral cells in most vertebrates, PNs in the *Drosophila* antennal lobe receive direct ORN input from a single glomerulus.

Circumstantial evidence suggests that interglomerular connections shape PN odor responses in *Drosophila*. A comparison of odor-evoked responses in ORNs and PNs corresponding to the same glomerulus revealed that the rank order of a PN's odor preferences can be different from the preferences of its presynaptic ORNs (Wilson et al., 2004). This argues that a PN's responses are not completely determined by its direct ORN inputs. Instead, it implies that PNs integrate input from multiple ORN types. However, this conclusion has been challenged by functional imaging studies (Ng et al., 2002; Wang et al., 2003).

Here, we use a variety of genetic manipulations and microdissections to remove direct ORN inputs to one or more glomeruli in the *Drosophila* antennal lobe. In vivo recordings from PNs postsynaptic to "silent" glomeruli reveal that these PNs receive lateral inputs from other glomeruli. The net effect of lateral synaptic inputs to PNs is predominantly excitatory and can be strong enough to trigger a train of action potentials. In order to define the functional connectivity between identified glomeruli, we have generated flies with only a single active ORN type. Stimulation of just one ORN type is sufficient to recruit lateral excitatory inputs to other glomeruli, but this sensitivity also leads to saturation as more ORN types are activated. A single glomerulus provides indirect excitatory input to most, if not all, glomeruli, thus defining a dense network of lateral connections spanning the entire antennal lobe. However, some lateral excitatory connections are substantially stronger than others. Finally, we find that this pattern of connection strengths is relatively stereotyped across flies, suggesting that it may be genetically hardwired. These findings directly demonstrate that synaptic crosstalk between glomeruli can shape PN odor responses in vivo. Furthermore, our results reveal some of the fundamental rules governing these interglomerular interactions.

RESULTS

Olfactory Stimuli Trigger Lateral Excitatory Interactions among Glomeruli

The *Drosophila* antennal lobes receive olfactory input from two peripheral organs, the antennae and the maxillary palps. The palps contain ~120 ORNs which fall into six distinct types not found in the antennae (de Bruyne et al., 1999; Goldman et al., 2005). The antennae contain an additional 43 ORN types not found in the palps (de Bruyne et al., 2001; Hallem et al., 2004). Thus, each glomerulus receives direct ORN input exclusively from either the palps or the antennae. Within the antennal lobe, the six palp glomeruli are intermingled with the 43 antennal glomeruli (Couto et al., 2005; Fishilevich and Vosshall, 2005). This anatomy provides a convenient way to independently manipulate inputs to two groups of glomeruli.

In order to determine whether interactions between glomeruli shape PN odor responses, we began by acutely severing the antennal nerves. This manipulation leaves the palp ORNs intact and allows us to test whether antennal PNs receive lateral input from palp glomeruli (Figure 1A). Consistent with previous reports (Berdnik et al., 2006), we found that ablating ORN input to some glomeruli does not induce morphological rearrangement of the remaining ORN axons, even five days postsurgery (Figure 1B). However, we cannot exclude the possibility that removing ORN input to some glomeruli induces more subtle synaptic plasticity of interglomerular connections. Therefore, we performed PN recordings immediately after severing the antennal nerves in order to rule out a role for any such plasticity.

Whole-cell patch-clamp recordings from PNs typically show abundant spontaneous synaptic input (Figure 1C). In contrast, PNs postsynaptic to antennal glomeruli in antennae-less flies show no spontaneous activity (Figures 1D and 1E). Nevertheless, odor stimulation of the maxillary palps evokes a depolarization in these PNs (n = 6 PNs in 6 flies; Figures 1D and 1E). The magnitude of this depolarization varied across cells but was sufficient to produce a train of spikes in a PN postsynaptic to glomerulus VC3, for example (Figure 1E). We confirmed that each of the PNs we recorded from innervated an antennal glomerulus by filling the cell with biocytin (see Experimental Procedures).

We averaged the membrane potential across six presentations of the same odor in the same cell (Figure 1F) before averaging across experiments (Figure 1G). All these odors strongly activate one or more palp ORN types (de Bruyne et al., 1999), and all elicited a substantial depolarization in each of the antennal PNs we recorded from. The solvent we use to dilute our odors (paraffin oil) evoked no response (Figure 1G). Removing both antennae and maxillary palps abolished odor-evoked depolarizations (n = 3), demonstrating that the maxillary palps mediate this response (Figure 1G).

These results demonstrate that antennal PNs receive lateral synaptic input from palp ORNs and that the net effect of this indirect input is excitatory. It is possible that some interglomerular synapses hyperpolarize PNs, but if so, this inhibition is evidently obscured by a larger excitatory component. It is important to note that ORN input was removed acutely (~10–20 min before recording). Therefore, the lateral excitation we observed cannot reflect remodeling of the antennal lobe circuitry.

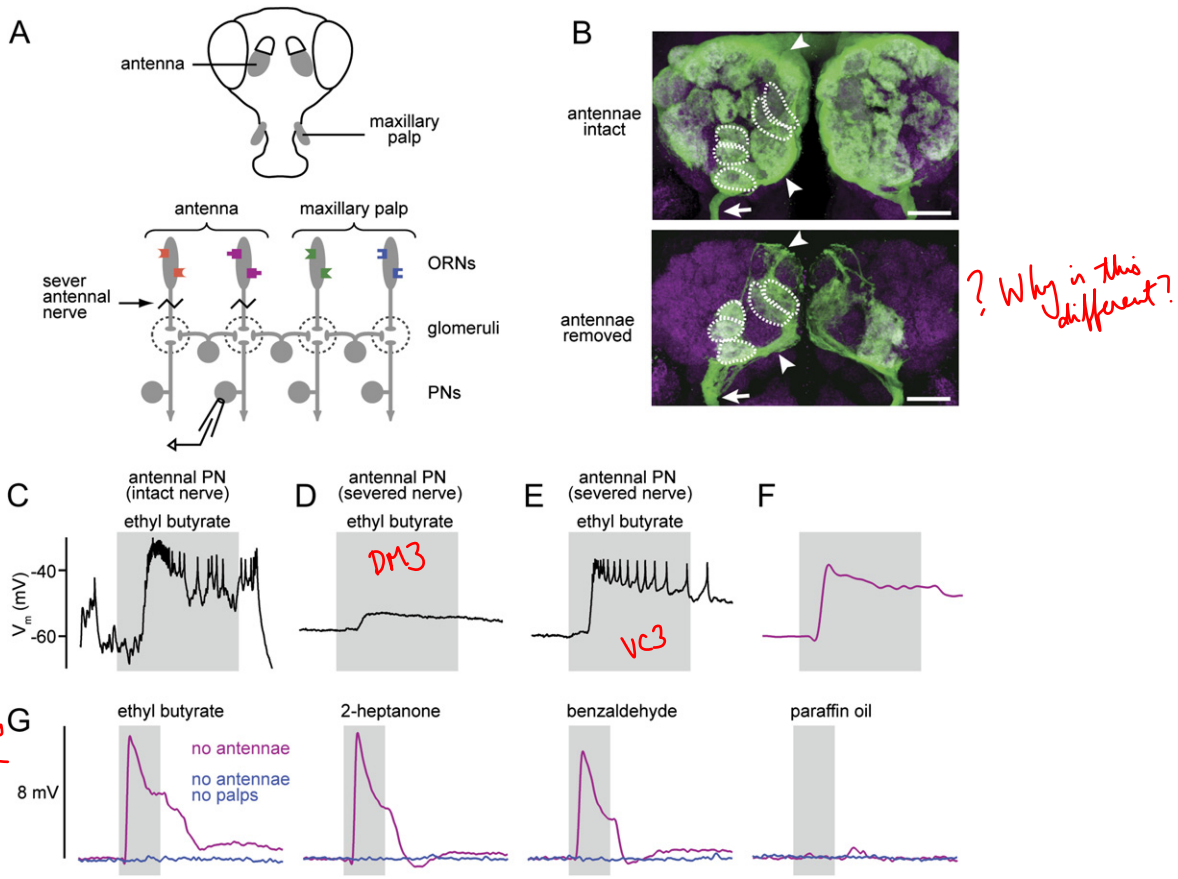

Figure 1. Olfactory Stimuli Trigger Excitatory Interactions among Glomeruli

(A) Both the antennae and the maxillary palps project to the antennal lobes. Severing the antennal nerves removes direct ORN input to antennal glomeruli but leaves input to palp glomeruli intact. Recording from a PN postsynaptic to a deafferented glomerulus reveals indirect input to that cell from palp ORNs.

(B) Axon targeting of palp ORNs is not altered by removing antennal ORNs. Projections of confocal stacks through the antennal lobes (neuropil in magenta) show ORN axons labeled with CD8:GFP (green). Glomeruli targeted by palp ORNs are outlined. Arrow indicates maxillary nerve. Arrowheads indicate axons projecting to or from the midline; each ORN projects bilaterally. Scale bars = 20 μm.

(C) With antennal nerve intact, a recording from an antennal PN (in glomerulus DM3) shows spontaneous and odor-evoked activity. Period of odor delivery is indicated by gray bar (500 ms).

(D) Recording from an antennal PN (in glomerulus DM3) after severing antennal nerves. Spontaneous activity is abolished, but a small odor-evoked depolarization remains.

(E) Recording from an antennal PN (in glomerulus VC3) after severing antennal nerves shows a large odor-evoked depolarization.

(F) Same as (E) but averaged across six trials with the same odor and low-pass filtered to remove spikes.

(G) Odor-evoked depolarizations averaged across all experiments with severed antennal nerves (magenta). No depolarization is observed when both antennae and maxillary palps are removed (blue). Note that this analysis pools data from six PNs corresponding to different antennal glomeruli.

Total Lateral Synaptic Excitation to a PN Is Substantial

What is the total impact of all lateral synaptic input to a PN? In order to answer this question, we selectively silenced a single ORN type. By recording from PNs postsynaptic to the "silent" glomerulus while stimulating the antennae and palps with odors, we should be able to observe the total lateral input to that PN.

In order to silence a single ORN type, we used flies with mutations in one of two odorant receptor genes, *Or43b* and *Or10a*. *Or43b* is expressed in ORNs that project to glomerulus VM2, and *Or10a* is expressed in ORNs that project to glomerulus DL1 (Couto et al., 2005; Fishilevich and Vosshall, 2005). The $Or43b^{1}$ null allele was produced by gene targeting and has been described previously (Elmore et al., 2003). The $Or10a^{f03694}$ allele results from a pBac insertion in the gene (Thibault et al., 2004) but has not been characterized previously. We first verified that this mutation does not disrupt ORN axon targeting (see Figure S1A in the Supplemental Data available with this article online). We then confirmed that both the $Or43b^{1}$ and $Or10a^{f03694}$ mutations virtually abolish ORN odor responses (Figures S1B–S1D). We occasionally observed very weak responses to a few specific odors in

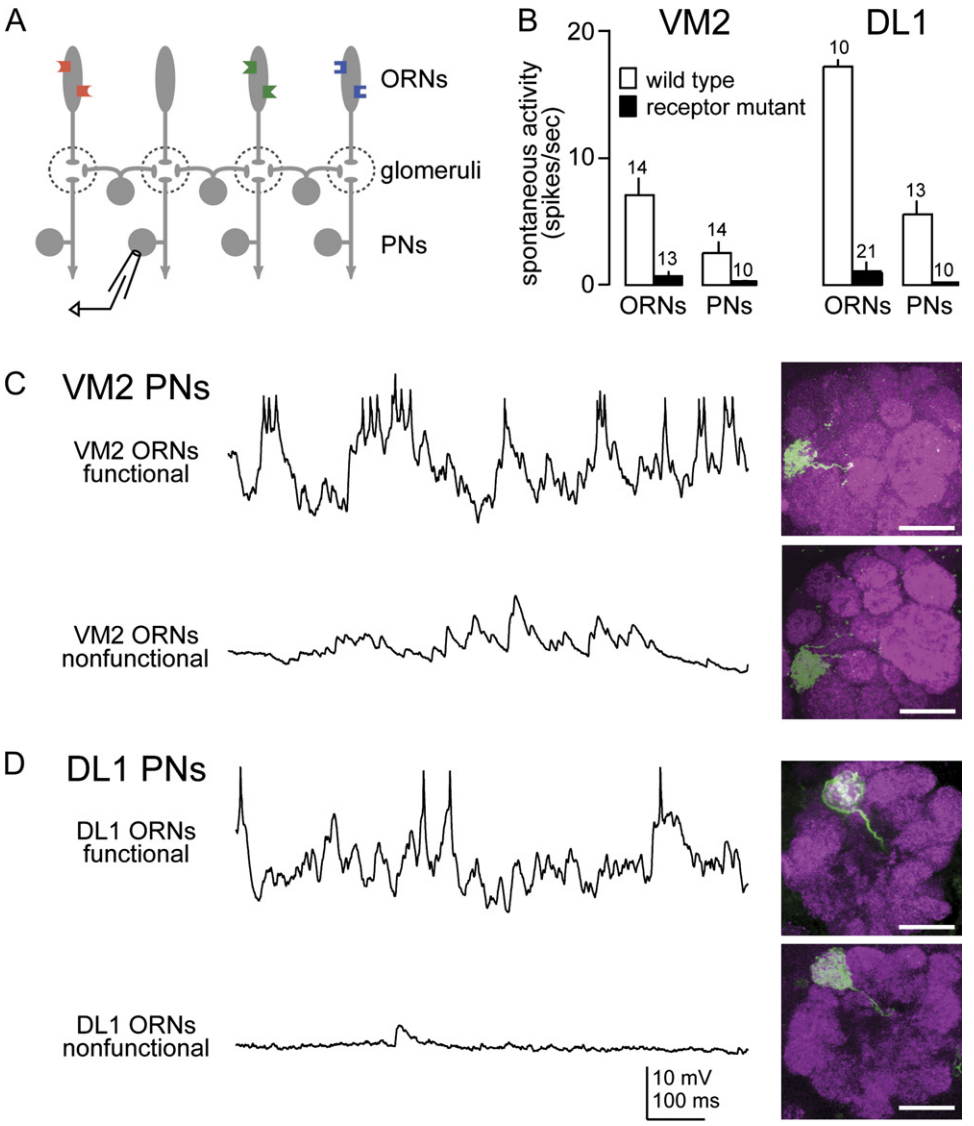

Figure 2. PNs Postsynaptic to "Silent" ORNs Show Reduced Activity but Normal Morphology

(A) Schematic of experiments in Figures 2–4: recording from PNs postsynaptic to ORNs lacking odorant receptors.

(B) Odorant receptor mutations reduce spontaneous activity in both ORNs and their postsynaptic PNs. Bars show mean ± SEM averaged across experiments, with n values above each bar ($p < 0.05$ for each wild-type/mutant comparison, t tests).

(C) Spontaneous electrophysiological activity and morphology of VM2 PNs in wild-type flies (top) and *Or43b*^{1} mutant flies (bottom). Images on the right are projections of confocal stacks through one antennal lobe (neuropil in magenta) showing the primary dendrite of the biocytin-filled PN (biocytin/streptavidin in green). The cell body and axon of the recorded PN are not present in these z sections. Scale bars = 20 μm. Lateral is to the right in both images.

(D) Spontaneous electrophysiological activity and morphology of DL1 PNs in wild-type flies (top) and *Or10a*^{f03694} mutant flies (bottom). Lateral is to the left in both images.

both mutants (Figure S2). These weak responses may be mediated by Or83b, a protein with homology to odorant receptors that is expressed in most ORNs and which is required for trafficking receptors to the cell membrane (Larsson et al., 2004). We did not use these odors in our stimulus set when we analyzed PN responses in these mutants (Figures 2–4). Note that these mutations also reduce the rate of spontaneous ORN spikes (Figure S1C).

We then recorded from PNs postsynaptic to these "silent" ORNs (Figure 2A). In flies with the mutation that silences VM2 ORNs, we targeted VM2 PNs using an enhancer trap line (Tanaka et al., 2004) to specifically label these cells with GFP (*NP5103-Gal4,UAS-CD8:GFP;Or43b*^{1}). We recorded from one PN per fly and confirmed the glomerular identity of each recorded PN by imaging the biocytin fill post hoc. As expected from

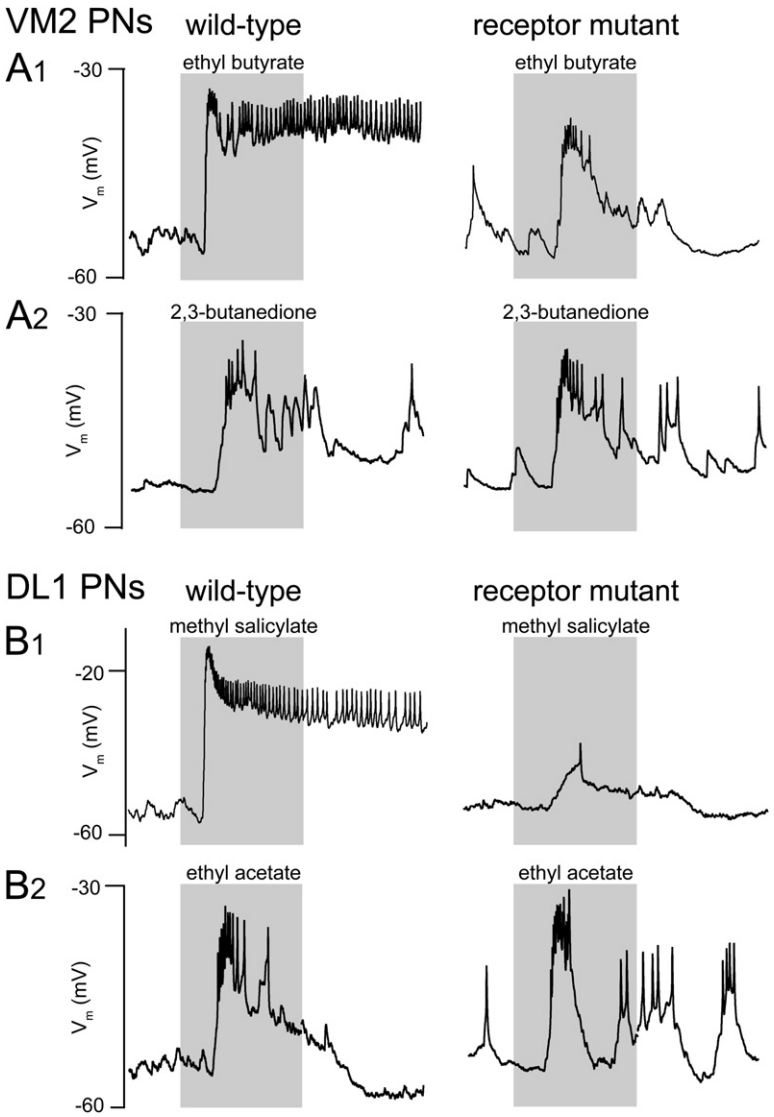

Figure 3. Comparing Odor Responses in PNs Postsynaptic to Normal versus "Silent" ORNs

Representative responses of PNs postsynaptic to wild-type ORNs (left column) and PNs postsynaptic to nonfunctional ORNs (right column). Most odors elicit a substantially larger response when presynaptic ORNs are functional (A_1, B_1). However, some odors elicit a similar response with or without functional presynaptic ORNs (A_2, B_2). Gray bars indicate the 500 ms period of odor stimulation. Transient stimulus artifacts from the olfactometer (at the end of the odor stimulus period) were blanked in some traces. Traces in the same row have the same y axis.

the decrease in spontaneous activity in mutant ORNs, spontaneous spiking in VM2 PNs was reduced compared to wild-type (Figures 2B and 2C). Similarly, in flies with mutant DL1 ORNs, we recorded from DL1 PNs using an enhancer trap line (Tanaka et al., 2004) to specifically label these cells with GFP (*Or10a^{f03694};+/+;NP3529-Gal4, UAS-nlsGFP*). Again, spontaneous spiking was reduced in these PNs (Figures 2B and 2D). We confirmed that these PNs show normal dendrite morphology in the absence of functional ORNs (Figures 2C and 2D), consistent with previous reports (Wong et al., 2002; Berdnik et al., 2006).

In flies with silent VM2 ORNs, all VM2 PNs were depolarized by every odor we tested (n = 10 cells in 10 flies), with the exception of 4-methyl phenol, which failed to elicit any activity in two cells. These depolarizations were typically large enough to trigger a train of action potentials (Figure 3). Similarly, in flies with silent DL1 ORNs, all DL1 PNs were depolarized by every odor we tested (n = 10 cells in 10 flies). Again, most responses were large enough to elicit a train of spikes. We also saw similar spiking responses to odors in cell-attached mode (prior to going whole-cell), demonstrating that these depolarizations are not an artifact of intracellular dialysis.

As expected, most odors evoked a larger response in wild-type flies than in mutant flies. For example, ethyl butyrate elicits vigorous activity in normal VM2 ORNs (Figure S1) and in wild-type VM2 PNs. When the VM2 ORNs are silenced, this odor elicits a much smaller response in VM2 PNs (Figure 3A_1). Similarly, methyl salicylate evokes a very strong response in DL1 ORNs (Figure S1) and in wild-type DL1 PNs but only a small response in DL1 PNs postsynaptic to silent ORNs (Figure 3B_1). We also noticed that in PNs postsynaptic to silent ORNs, odor-evoked responses were often more transient than in wild-type PNs (Figures 3A_1 and 3B_1).

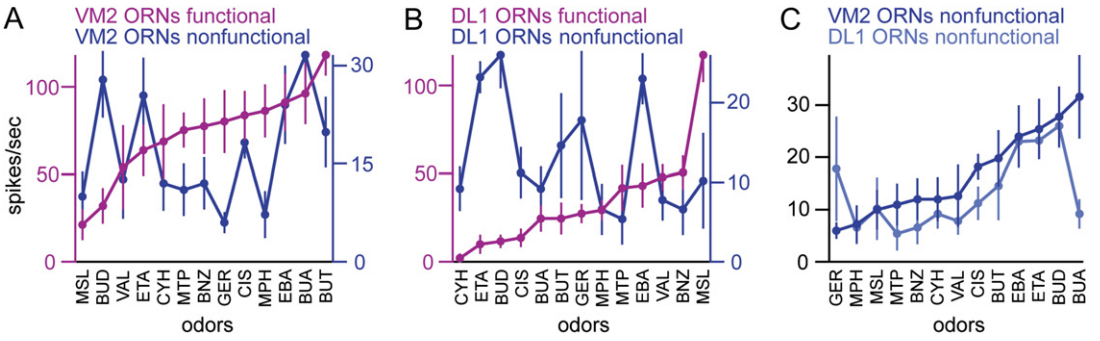

Figure 4. Odor Tuning of PN Responses Postsynaptic to Normal versus "Silent" ORNs

(A and B) Tuning curves comparing odor responses of PNs postsynaptic to wild-type (magenta) and mutant ORNs (blue). PNs are postsynaptic to glomerulus VM2 (A) or DL1 (B). Each point represents firing rate over the 500 ms odor stimulus period, averaged across experiments (mean ± SEM). Note different y scales for magenta and blue symbols. Odors are arranged so the smallest wild-type responses are on the left and the largest are on the right. See Experimental Procedures for odor abbreviations.

(C) Tuning curves comparing odor responses of VM2 and DL1 PNs postsynaptic to mutant ORNs. Note correlated but not identical odor tuning.

Some odor responses, however, were relatively unaffected by odorant receptor mutations. For example, 2,3-butanedione evokes very little response in wild-type VM2 ORNs (Figure S1). When these ORNs are silenced, the response of VM2 PNs to this odor is virtually unaltered (Figure 3A$_2$). Similarly, ethyl acetate does not excite wild-type DL1 ORNs (Figure S1). Accordingly, the response of DL1 PNs to ethyl acetate is undiminished by silencing their presynaptic ORNs (Figure 3B$_2$).

How does the size of total lateral input to a PN depend on the odor stimulus? We quantified odor responses by computing mean firing rates over the 500 ms duration of the odor stimulus, and we plotted these response magnitudes for each odor stimulus to produce tuning curves (Figures 4A and 4B). These plots show that different odors evoke different amounts of lateral excitatory input to each PN. However, the odor tuning of PNs postsynaptic to silent ORNs is completely different from the normal odor tuning of these PNs. For both glomeruli, the odor tuning of wild-type and mutant PNs showed no significant correlation (both comparisons Pearson's $r^2 < 0.05$, $p > 0.4$).

We also noted that, in the absence of direct ORN inputs, both VM2 PNs and DL1 PNs are broadly tuned to odors. This suggests that each of these glomeruli receives indirect excitatory input from multiple ORN types, not just one or two. We wondered whether these two glomeruli receive indirect input from similar or different populations of ORNs. To assess this, we compared the responses of PNs in these two "silent" glomeruli to the same odors. Overall, the responses of these two PN types are significantly correlated (Figure 4C; Pearson's $r^2 = 0.31$, $p < 0.05$). However, some odors elicit different amounts of lateral input to these glomeruli. For example, butyric acid elicits a larger response in VM2 than in DL1 ($p = 0.05$, t test, $n = 6$ for each glomerulus). These results are consistent with the idea that these two glomeruli receive indirect input from overlapping populations of ORNs but that the indirect inputs to these PNs are not identical.

Characterizing Lateral Input to Many Glomeruli Originating from a Single Glomerulus

Because total lateral excitatory input to VM2 and DL1 PNs is broadly tuned and significantly correlated, it is likely that two glomeruli receive indirect input from many of the same ORNs. This, in turn, implies that each ORN type provides indirect input to many glomeruli. To test this prediction directly, we designed experiments to measure the spread of excitation across the antennal lobe evoked by activation of a single ORN type. We used two approaches to selectively stimulate one ORN type (Figure 5). These two approaches have complementary strengths and weaknesses but yielded similar results. In the first method (experiment 1), we took advantage of a mutation in *Or83b*. This gene is expressed in most ORNs and encodes a chaperone protein required for trafficking odorant receptors to ORN dendrites (Larsson et al., 2004; Benton et al., 2006). Mutating *Or83b* abolishes odor responses in all maxillary palp ORNs (and many antennal ORNs; Figure S3). Thus, all ORN input to the antennal lobes is abolished by removing the antennae of mutant flies. In these flies, we then rescued normal function in the maxillary palp ORNs that project to glomerulus VA7l. This was done by expressing *Or83b* under the control of the odorant receptor gene promoter corresponding to the VA7l ORNs (*Or46-Gal4/UAS-Or83b;Or83b*^{2}; Fishilevich and Vosshall, 2005). We verified the specificity of this rescue by making extracellular ORN recordings from the maxillary palps. Each sensillum in the palp contains exactly two ORNs, and a VA7l ORN is always paired with an ORN that projects to another glomerulus (de Bruyne et al., 1999; Goldman et al., 2005). In the palps of "rescued" flies, we encountered only silent sensilla, or sensilla containing exactly one spontaneously active ORN ($n = 51$ sensilla). This ORN always displayed odor tuning that matched the odor tuning of wild-type VA7l ORNs (Figures 5B and S4). We verified that the rescued ORNs correctly target glomerulus VA7l by coexpressing CD8:GFP with Or83b (Figure 5C). Furthermore, biocytin fills show that

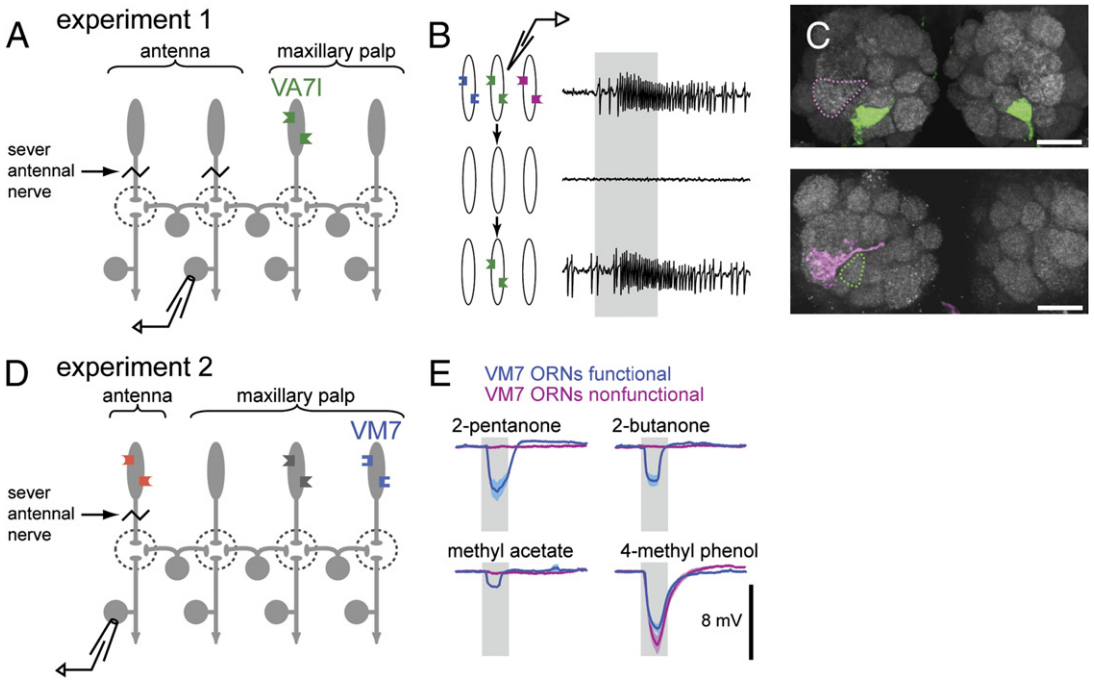

Figure 5. Two Strategies for Stimulating a Single ORN Type

(A) In experiment 1, only one maxillary palp ORN type (VA7l) has functional odorant receptors. Antennal nerves are severed. Recordings are performed from PNs postsynaptic to antennal glomeruli.

(B) Genetic strategy to limit functional odorant receptors to a single type of ORN. Top, single-sensillum recording from wild-type ORN projecting to glomerulus VA7l (the second ORN in this sensillum has been killed with diphtheria toxin to show only the VA7l ORN spikes; see Table S1). Middle, in the *Or83b*^{2} mutant, all spontaneous and odor-evoked activity is eliminated from maxillary palp ORNs. Bottom, odor response is rescued in VA7l ORNs by selective expression of Or83b in these neurons. Gray bar = 500 ms puff of methyl salicylate.

(C) Both ORNs and PNs show correct glomerular targeting in flies with "rescued" VA7l ORNs. Top, projection of a confocal stack through antennal lobes of a fly with rescued VA7l ORNs. VA7l ORNs are labeled with CD8:GFP (green). A neighboring glomerulus (VA1v) is outlined in magenta. Bottom, biocytin-fill of a VA1v PN (magenta) recorded in a fly with rescued VA7l ORNs where all other ORNs are nonfunctional. This PN does not invade glomerulus VA7l (green). Scale bars = 20 μm.

(D) Experiment 2 uses a restricted odor set to selectively stimulate VM7 ORNs. Antennal nerves are severed, and the Δ*85* mutation is used to reduce ORN activity in two maxillary palp ORN types. Recordings are performed from PNs postsynaptic to antennal glomeruli.

(E) A restricted odor set activates only VM7 ORNs. Local field potential recordings from the maxillary palp of flies with either functional (blue; genotype +/+;Δ*85*) or nonfunctional VM7 ORNs (magenta; genotype *Or42a*^{f04305};Δ*85*). Responses are only present when VM7 ORNs are functional. As a positive control, we confirmed that 4-methyl phenol elicits a robust response in both genotypes; this odor activates several maxillary palp ORNs that are functional in both genotypes. Traces are mean ± SEM, averaged across experiments (n = 3 for each genotype).

PNs postsynaptic to neighboring glomeruli do not inappropriately invade glomerulus VA7l (Figure 5C). This argues that the antennal lobe circuitry is grossly normal in the *Or83b*^{2} mutant.

This approach permits us to selectively stimulate exactly one ORN type. However, it has the drawback that most ORN types are inactive during the development of the fly, which could conceivably produce subtle changes in the antennal lobe circuitry. To address this issue, we used a second method to stimulate one ORN type under conditions in which almost all ORNs are normal and active throughout the life of the fly; this ensures that normal antennal lobe circuitry is preserved. In this approach (experiment 2, Figure 5D), we sought to identify a panel of odors that only stimulates one ORN type. Because most ORNs respond to many different odors, it is difficult to find such an odor set. To simplify the problem, we cut the antennal nerves just prior to recording, leaving only the six maxillary palp ORN types. Additionally, we used flies bearing the Δ*85* mutation, which abolishes most odor responses in two of the six maxillary palp ORN types (Figures S5 and S6). Thus, in antennae-less flies in a Δ*85* background, there are only four functional maxillary palp ORN types. We screened a large panel of odors and identified a set of 14 that exclusively stimulates the VM7 ORNs while evoking no response from the other three functional ORN types in this genotype. This is demonstrated by local field potential recordings from the maxillary palp. When VM7 ORNs are functional, all odors in this set evoke a local field potential response. These responses are abolished by the *Or42a*^{f04305} mutation (Thibault et al., 2004), which renders VM7 ORNs nonfunctional (Figure 5E; see also Figures S5 and S6). In summary, both experiments 1 and 2 permit selective stimulation of one ORN type.

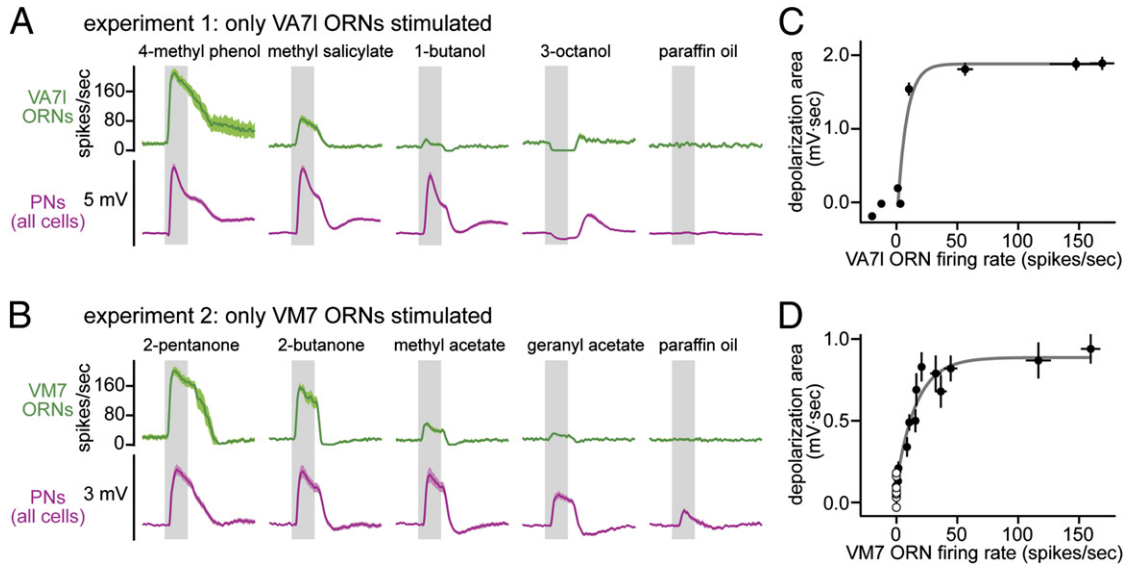

Figure 6. Odor Stimulation of One ORN Type Evokes Lateral Input to Many PNs

(A) Experiment 1. Top, peristimulus-time histograms show odor responses of VA7l ORNs (n = 5). Bottom, average depolarizations recorded in PNs postsynaptic to glomeruli lacking direct ORN input (n = 72).

(B) Experiment 2. Top, peristimulus-time histograms showing odor responses of VM7 ORNs (n = 6). Bottom, average depolarizations recorded in PNs postsynaptic to glomeruli lacking direct ORN input (n = 15).

(C) Experiment 1. Average depolarization area plotted versus VA7l ORN firing rate. Each point represents a different odor. Curve is an exponential fit (only excitatory ORN responses are included in fit).

(D) Experiment 2. Average depolarization area plotted versus VM7 ORN firing rate for each odor (solid symbols). Curve is an exponential fit. In flies lacking functional VM7 ORNs (open symbols), odor-evoked depolarizations are virtually absent ($Or42a^{f04305}$;Δ*85*; n = 3).

All panels: values are mean ± SEM, averaged across experiments.

In experiment 1 (genetically rescuing VA7l ORNs), we recorded from a total of 72 PNs postsynaptic to nonrescued glomeruli. PNs were selected at random from the dorsal cluster of PN cell bodies in the antennal lobe. Only one PN was recorded in each fly, which allowed us to unambiguously determine the glomerular identity of each PN after filling it with biocytin. Together, these 72 PNs targeted 24 out of the 49 glomeruli in the antennal lobe. In every one of these PNs, we observed a depolarization while stimulating the VA7l ORNs with odors. This implies that the VA7l ORNs broadcast indirect excitatory input to most glomeruli. As expected, the tuning of the lateral excitatory input to PNs always reflected the tuning of the VA7l ORNs (Figure 6A). Odors that excited VA7l ORNs produced depolarizations in PNs, whereas inhibition of VA7l ORNs led to a small hyperpolarization. This hyperpolarization probably represents an interruption in tonic lateral excitation driven by spontaneous action potentials in VA7l ORNs.

In experiment 2 (selective odor stimulation of VM7 ORNs), we recorded from a total of 15 PNs. We observed odor-evoked depolarizations in every one of these PNs. This suggests that the VM7 ORNs send lateral excitation indirectly to most glomeruli. And as expected, the tuning of the lateral excitatory input always reflected the tuning of the VM7 ORNs (Figure 6B). The average magnitude of this depolarization was about half of that observed in experiment 1.

In both experiment 1 (VA7l-only) and experiment 2 (VM7-only), the magnitude of lateral depolarization did not scale linearly with ORN firing rate. Odors that evoked only a small ORN response produced a near-maximal lateral depolarization in PNs. Odors that evoked a larger ORN response saturated the lateral circuitry. This is shown by plotting the area under the membrane potential deflection (computed after low-pass filtering the membrane potential) versus ORN firing rate (Figures 6C and 6D). The nonlinearity of these curves illustrates both the sensitivity and the saturation of interglomerular excitatory circuits. To confirm that the lateral depolarizations in experiment 2 are driven by the VM7 ORNs, we combined the Δ*85* mutation with an odorant receptor gene mutation that silences the VM7 ORNs ($Or42a^{f04305}$;Δ*85*). In this genotype, we saw essentially no odor responses in any PNs (Figure 6D, open circles, n = 3).

These results demonstrate that ORN inputs from one glomerular processing channel can easily saturate the lateral excitatory circuitry of the antennal lobe. How are inputs from multiple ORN types integrated by this circuitry? We used an odor blend to investigate how odor-evoked signals from two ORN inputs are combined. In antennae-less Δ*85* flies, the odor 2-butanone (10^{-5} dilution) activates only the VM7 ORNs (Figure 5E), while the odorant methyl salicylate (10^{-2} dilution) activates only the VA7l ORNs (data not shown). In isolation, these stimuli

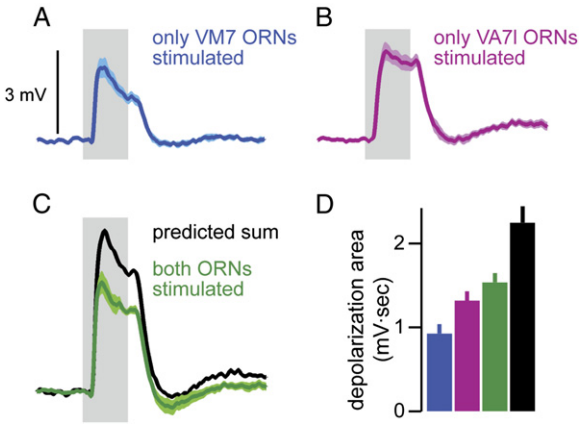

Figure 7. Lateral Excitatory Circuits Sublinearly Summate Inputs from Multiple ORN Types

(A) Average depolarization evoked in antennal PNs by selective stimulation of VM7 ORNs with 2-butanone (10^{-5} dilution) in Δ*85* flies.

(B) Average depolarization evoked in antennal PNs by selective stimulation of VA7l ORNs with methyl salicylate (10^{-2} dilution) in Δ*85* flies, recorded from the same PNs as in (A).

(C) Comparing the average depolarization evoked by simultaneous stimulation of both ORN types (green), versus the predicted linear sum of stimulating each ORN type alone (black).

(D) Depolarization quantified as the area under the membrane potential deflection.

All panels: values are mean ± SEM, averaged across eight PNs recorded in different flies. All PNs were postsynaptic to glomeruli DL5, DM6, or VM2. Vertical scaling is the same in (A)–(C).

appear to saturate the lateral excitatory circuitry of the antennal lobe: stimulating VM7 PNs with 2-butanone evokes a maximal lateral depolarization in experiment 2 and stimulating VA7l PNs with methyl salicylate evokes a maximal lateral depolarization in experiment 1 (Figure 6, magenta traces). What happens when these two inputs are integrated? When we blended the two odors to stimulate both VA7l and VM7 ORNs simultaneously in antennaeless Δ*85* flies, we observed lateral depolarizations that were significantly larger than the response to either odor alone (Figure 7; $p \leq 0.01$ for both comparisons, n = 8 PNs, paired t tests). This shows that multiple ORN inputs are effectively integrated by the lateral excitatory circuitry of the antennal lobe. However, the response to the blend was significantly smaller than that predicted by a linear sum of the responses evoked by stimulating each ORN type individually (Figure 7; $p < 10^{-4}$, paired t test). This demonstrates that saturation occurs across ORN input channels, not just within an ORN input channel.

For a given ORN input (either VA7l or VM7), different PNs showed substantially different amounts of lateral depolarization in response to the same odor. In experiment 1, for example, the response evoked by the strongest odor (4-methyl phenol) ranged from 1.7 mV to 11.8 mV. Responses in some PNs were large enough to elicit a few spikes, but responses in other PNs responses were much weaker. This suggests that different PNs receive different amounts of lateral excitatory input from any given glomerulus. Are these connections random, or are they a stereotyped function of glomerular identity? To address this question, we compared the responses of PNs corresponding to the same glomeruli recorded in different flies. In our data set from experiment 1, there were 11 glomeruli that we hit at least three times. In experiment 2, we recorded selectively from PNs in only three glomeruli by using an enhancer trap line to label these cells with GFP (*NP3481-Gal4,UAS-CD8:GFP;+/+;Δ85*). This allowed us to obtain multiple recordings from the same PN type.

Overall, we found that the strength of lateral excitatory connections was relatively stereotyped across flies. In quantitative terms, differences we observed between glomeruli were larger than the variability we observed for a given glomerulus across flies. For example, in experiment 1, selective stimulation of VA7l ORNs produced a significantly greater depolarization in VC4 PNs compared to VA1v PNs (Figures 8A–8C; $p < 0.05$; VC4, n = 7; VA1v, n = 8). In experiment 2, selective stimulation of VM7 ORNs produced a significantly greater depolarization in glomerulus DL5 than in glomerulus VM2 or DM6 (Figures 8D–8F; $p < 0.05$; DL5, n = 5; VM2, n = 3; DM6, n = 7). We also noted that the nonlinear relationship between the lateral depolarization and ORN firing rate had a similar sensitivity and exponential shape across different glomeruli; it is the saturation level that differs (Figures 8B and 8E). Together, these results demonstrate that the amount of lateral excitatory input to a PN depends on the identity of the glomerulus where its dendrite is located. The magnitude of lateral depolarization is not correlated with the input resistance of the cell (Pearson's $r^2 = 0.027$), ruling out one trivial explanation for this systematic difference.

We next asked whether the magnitude of glomerular crosstalk varied systematically with distance. Figure 9 shows the relative connection strength for all 24 glomeruli we recorded from in experiment 1, mapped in relation to the location of the only glomerulus receiving direct ORN input (VA7l). Connection strength is defined as the relative response to 4-methyl phenol, which is the strongest stimulus in our odor set for the VA7l ORNs. This map illustrates that there is no obvious relationship between interglomerular distance and the strength of lateral excitatory connections. We also asked if there is a correlation between connection strength and the morphological class of the ORN type corresponding to each glomerulus. Previous studies have shown that ORNs housed in the three major morphological classes of sensilla (basiconic, coeloconic, and trichoid) tend to project to nearby glomeruli and therefore define several zones in the antennal lobe (Couto et al., 2005; Fishilevich and Vosshall, 2005). Figure 9B shows that the zones defined by these sensillum classes receive similar overall levels of lateral excitation. Finally, we tested whether there is a relationship between the odor tuning of the normal ORN input to a glomerulus and the strength of excitatory lateral input it receives from VA7l. Comprehensive odor-tuning data for 16 of the colored glomeruli in Figure 9A has been

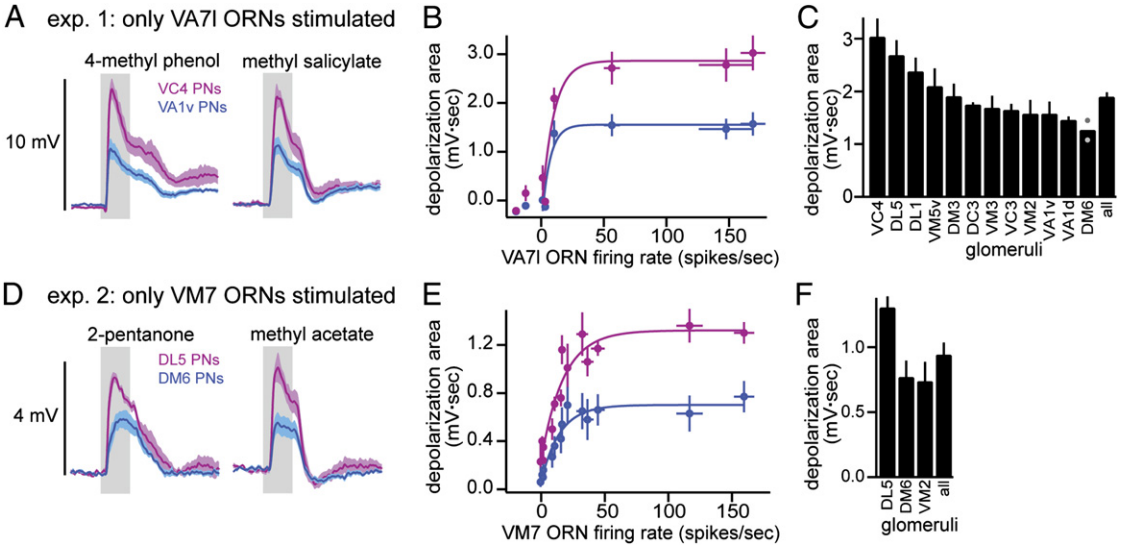

Figure 8. The Strength of Lateral Connections Is Heterogeneous and Stereotyped across Flies

(A) Experiment 1. Stimulation of VA7l ORNs evokes different levels of lateral depolarization in PNs postsynaptic to two different glomeruli (magenta = VC4, blue = VA1v).

(B) Depolarization area in these PNs is plotted versus VA7l ORN firing rate for each odor. Curves are exponential fits (only excitatory ORN responses are included in fit).

(C) Comparing lateral depolarization in all PN types that we recorded from at least three times (except DM6 where n = 2, gray dots). Graph shows average response to 4-methyl phenol in these PNs.

(D) Experiment 2. Stimulation of VM7 ORNs evokes different levels of lateral depolarization in PNs postsynaptic to two different glomeruli (magenta = DL5, blue = DM6).

(E) Depolarization area in these PNs is plotted versus VM7 ORN firing rate for each odor. Curves are exponential fits.

(F) Comparing lateral depolarization area in three different glomeruli ($n \geq 3$ for each). Graph shows average response to 2-pentanone for each glomerulus.

All panels: values are mean ± SEM, averaged across experiments.

compiled by other investigators (Hallem and Carlson, 2006). We used this data set to compute the correlation coefficient (Pearson's r) between ORN odor responses for every pairwise combination of these 16 glomeruli and then plotted the difference in lateral depolarization for each pair as a function of this correlation. We found there is no relationship between glomerular tuning and depolarization strength (Figure 9C).

DISCUSSION

In this study, our goal was to observe the synaptic inputs to PNs arising from local antennal lobe circuits. We have used a variety of complementary strategies to remove direct ORN input to the PN we were recording from, meanwhile leaving other ORNs intact. These manipulations allowed us to directly observe lateral excitatory input to a PN originating from other glomeruli.

It is important to emphasize that this lateral excitation cannot be ascribed purely to compensatory rearrangement of the antennal lobe circuitry. This point is most forcefully demonstrated by experiments in which most or all ORNs are normal and active until we sever the antennal nerves immediately before recording (Figures 1 and 6B). In these experiments we recorded from PNs 10–20 min after removing the antennae and always observed odor-evoked lateral depolarizations. Hence, the circuitry mediating these responses must exist in normal flies prior to removing antennal input.

An Individual PN Integrates Lateral Inputs from Many ORN Types

Excitatory connections between glomeruli appear to be very dense, perhaps all-to-all. This conclusion is supported by four pieces of evidence. First, the magnitude of the depolarization we observed when almost all ORNs are intact (Figures 2–4) is larger than that observed when only the maxillary palp ORNs are intact (Figure 1), which in turn is larger than that observed when only a single ORN type is intact (Figures 5–9). This argues that most PNs receive indirect input from many ORN types. Second, when we restricted ORN input to a single glomerulus, every PN we recorded from (87 of 87 cells) received at least weak lateral input from that glomerulus. This implies that each ORN type broadcasts indirect input to most or all glomeruli. Third, the odor tuning of the total lateral input to a glomerulus is much broader than the odor tuning of a typical ORN. Fourth, the lateral input to VM2 PNs and DL1 PNs has a relatively similar (though not identical) odor-tuning profile. This suggests that large and

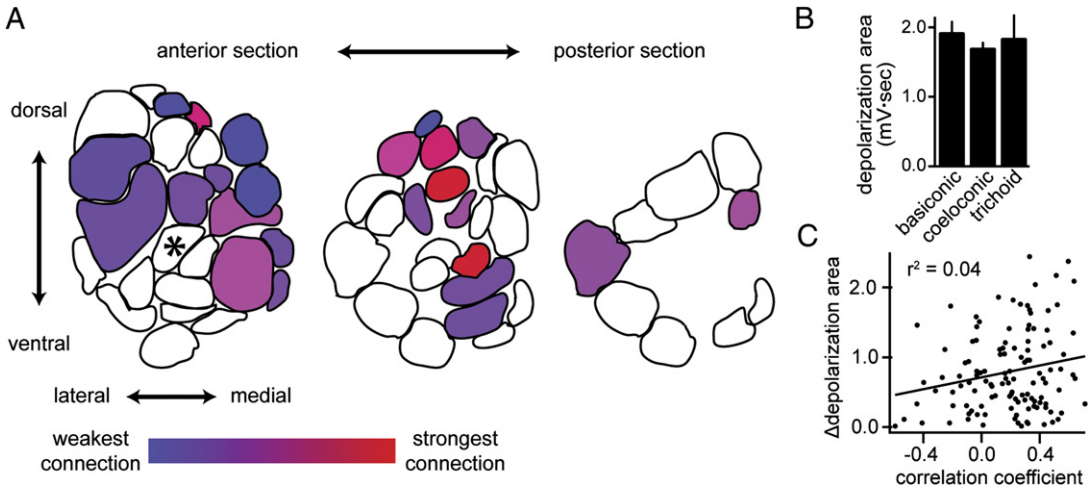

Figure 9. Lateral Excitation Is Broadly Distributed throughout the Antennal Lobe

(A) Schematic representation of all glomeruli in the antennal lobe, represented as three sections through the fly's right lobe (modified from Laissue et al. [1999]). Color indicates average relative depolarization measured in PNs postsynaptic to each glomerulus during selective stimulation of VA7l ORNs. Asterisk marks glomerulus VA7l. We did not sample PNs postsynaptic to white glomeruli.

(B) Glomeruli postsynaptic to different morphological types of sensilla receive similar levels of lateral input. Graph compares average depolarization area (±SEM) evoked by 4-methyl phenol in glomeruli targeted by ORNs in basiconic sensilla (n = 14 glomeruli), coeloconic sensilla (n = 3 glomeruli), and trichoid sensilla (n = 6 glomeruli). Data on morphological types were taken from Couto et al. (2005).

(C) There is no relationship between odor tuning and strength of lateral input. Comprehensive odor-tuning data for 16 ORN types was taken from Hallem and Carlson (2006). For every possible pairwise combination of 16 glomeruli, the difference in the average lateral depolarization evoked by 4-methyl phenol in these two PN types is plotted versus the correlation between the odor tuning of the ORN inputs to those glomeruli.

overlapping populations of ORNs provide indirect input to these two types of PNs. All-to-all connectivity is a parsimonious explanation for all these observations.

A Specific Matrix of Excitatory Connections

It should be noted that although lateral excitatory connectivity is dense and perhaps all-to-all, it is nevertheless selective. When we stimulated a single ORN type and recorded sequentially from PNs in different glomeruli, we found that each PN type receives a characteristically strong or weak lateral input from that ORN type. Furthermore, these characteristic connection strengths are relatively stereotyped across flies. This suggests that the synaptic connectivity of local interneurons in the antennal lobe may be genetically hardwired.

Notably, the strength of these lateral excitatory connections is not correlated with the distance between the target glomerulus and the location of the ORN inputs. This means that the spatial relationship between glomeruli does not limit the strength of their lateral interactions. This finding also argues that lateral excitation does not reflect spillover of excitatory neurotransmitter from the glomerulus receiving active ORN input, since in this case PNs closer to the active glomerulus would be expected to see a larger depolarization.

There is some tension between the idea that excitatory connection strengths between glomeruli are varied and the finding that VM2 and DL1 PNs see similarly tuned total lateral excitatory input. One possibility is that the lateral inputs to VM2 and DL1 PNs just happen to be unusually well correlated. Another possibility is that a given target glomerulus receives characteristically strong (or characteristically weak) indirect inputs from all ORN types. In this latter scenario, the strength of the lateral depolarization would vary across glomeruli, but its odor tuning would not.

Sensitivity and Saturation of Lateral Excitatory Circuits

The lateral excitatory circuits of the antennal lobe are remarkably sensitive to small levels of afferent input. We have shown that activating ORNs presynaptic to a single glomerulus produces a substantial lateral depolarization in many or all PNs. Moreover, the magnitude of the lateral depolarization arising from a single ORN type is extremely sensitive to small increases in ORN firing rate. Even an odor that evokes a very weak response in these ORNs (e.g., 1-butanol or geranyl acetate in Figure 6) still evokes substantial lateral excitation.

Another striking feature of lateral excitatory circuits is their saturability. In experiments where we stimulated only one ORN type, increasing the rate of incoming ORN spikes from 50 to 150 spikes/second had little effect on the amount of lateral excitatory input that was broadcast to other glomeruli. Furthermore, in experiments where we stimulated two ORN types, the combined effect of these two input channels was substantially less than the sum of each channel when stimulated individually. This type of saturation should tend to limit the magnitude of lateral excitatory synaptic input to a PN.

Together, these results suggest that the impact of lateral excitatory connections might be strongly dependent on odor concentration. Testing this hypothesis will require comparing the sensitivity of direct and lateral inputs to a range of concentrations and understanding how these inputs are integrated by PNs.

A Cellular Substrate for Lateral Excitatory Connections

While this manuscript was under review, a report appeared that identified a novel population of cholinergic local neurons in the *Drosophila* antennal lobe (Shang et al., 2007). There is no direct evidence that these local neurons mediate the local excitatory connections we have observed, but this hypothesis seems plausible. Each cholinergic local neuron reportedly innervates most glomeruli, and this morphology could easily explain our observation that a single ORN type broadcasts excitatory input to most or all PNs. Interestingly, excitatory (glutamatergic) local neurons were also recently identified in the olfactory bulb (Aungst et al., 2003), although it is not known whether these cells make synapses onto mitral cells, the analog of antennal lobe PNs.

Shang et al. (2007) also independently provided evidence that PNs receive lateral excitatory input. As in our study (Figures 2–4), these investigators measured activity in PNs whose presynaptic ORNs have been silenced by an odorant receptor gene mutation. Complementary to our electrophysiological approach, Shang et al. (2007) used a genetically-encoded ecliptic pHluorin to monitor the balance of synaptic vesicle exocytosis and endocytosis at presynaptic sites in PN dendrites. They found that PNs whose presynaptic ORNs were silent still showed odor-evoked dendritic synaptopHluorin signals, implying that these PNs receive indirect excitatory input from other ORNs.

Lateral Inhibition in the *Drosophila* Antennal Lobe

Models of olfactory processing in the insect antennal lobe and the vertebrate olfactory bulb stress the importance of inhibitory connections between glomeruli (Mori et al., 1999; Laurent, 2002). What about lateral inhibition in the *Drosophila* antennal lobe? It is known that GABAergic interneurons ramify throughout the *Drosophila* antennal lobe and release GABA in response to odor stimulation (Stocker et al., 1997; Ng et al., 2002; Wilson and Laurent, 2005). *Drosophila* antennal lobe PNs have $GABA_A$-like and $GABA_B$-like receptors, and antagonists of these receptors disinhibit PN odor responses (Wilson and Laurent, 2005). Given this, it is perhaps surprising that we have not observed lateral synaptic inhibition in PNs.

Several considerations put this finding in perspective. First, although the lateral inputs we observe are dominated by excitation, it is possible that these responses reflect the integration of both excitatory and inhibitory inputs. As a result, inhibition could be masked by a larger postsynaptic excitation. Second, although our results are inconsistent with a dominant role for interglomerular postsynaptic inhibition of PNs, our findings do not preclude a role for interglomerular presynaptic inhibition of ORN axon terminals. Presynaptic inhibition of neurotransmitter release from ORN axons is a well-known phenomenon in the mammalian olfactory bulb (Ennis et al., 2001; McGann et al., 2005; Murphy et al., 2005; Wachowiak et al., 2005) and in the crustacean olfactory lobe (Wachowiak et al., 2002). In this study, we abolished or severely reduced direct ORN input to the PNs we were recording from, which necessarily prevents us from observing any substantial presynaptic inhibition.

It is worth noting that neither $GABA_A$ nor $GABA_B$ receptors can mediate the lateral depolarization we observe. Both $GABA_A$ and $GABA_B$ conductances are hyperpolarizing in PNs (Wilson and Laurent, 2005). And although $GABA_A$ and $GABA_B$ receptor antagonists together completely block GABA-evoked hyperpolarizations in PNs (Wilson and Laurent, 2005), they do not diminish the lateral depolarization we describe in this study (Figure S7). This result also demonstrates that the lateral depolarization does not represent disinhibition (inhibition of inhibitory input to PNs).

Implications of Lateral Excitatory Connections for Odor Processing

A significant transformation in odor responses occurs between the ORN and PN layer in the *Drosophila* olfactory system. First, the odor tuning of PNs can be broader than the odor tuning of their presynaptic ORNs (Wilson et al., 2004). This may reflect, in part, the effects of the lateral excitatory connections we have described in this study. Because we have observed that the odor tuning of lateral input to a PN is different from the odor tuning of its direct ORN input, it seems likely that these lateral inputs promote excitatory responses to odors that would not have otherwise excited that PN. A second feature of the ORN-to-PN transformation is that the rank order of PN odor preferences can differ from the odor preferences of their presynaptic ORNs (Wilson et al., 2004). Again, because the odor tuning of lateral input to a PN is different from the odor tuning of its direct ORN input, it seems likely that lateral excitatory connections between glomeruli contribute to this phenomenon.

However, it would be misleading to neatly assign different components of a PN's odor response to direct versus lateral excitatory inputs. Direct and lateral excitation may coexist with pre- and postsynaptic inhibition, and all these inputs are likely to be integrated by PNs in a nonlinear fashion. Broad tuning in PNs could also reflect some nonlinearity in ORN-to-PN connections.

In general, bridging the gap between cellular and systems neuroscience will require a deeper understanding of how neurons integrate complex synaptic inputs in vivo. Using a combination of genetic techniques and in vivo electrophysiology, we have begun to dissect the various synaptic interactions involved in odor processing in the *Drosophila* antennal lobe. Our strategy has been to eliminate one input to an identified neuron in order to

unmask other relevant interactions. Here, this approach has revealed broadly distributed but specific excitatory connections between glomeruli. Although the behavior of a neural circuit is ultimately a complex product of its components, some insight can nevertheless be gained by manipulating one element at a time, provided that appropriate genetic tools are available. In this respect, the *Drosophila* olfactory circuit represents a powerful system for understanding the synaptic and cellular computations performed on sensory stimuli that ultimately produce perception and behavior.

EXPERIMENTAL PROCEDURES

Fly Stocks

Flies were reared at room temperature on conventional cornmeal agar. All experiments were performed on adult female flies 2–7 days post-eclosion. Fly stocks were kindly provided as follows: *Or10a-Gal4* (Barry Dickson); *Or43b*^{1} (Dean Smith); *NP5103-Gal4*, *NP3529-Gal4*, and *NP3481-Gal4* (Kei Ito and Liqun Luo); *UAS-Or83b*, *Or83b-Gal4*, *Or83b*^{2}, *Or46a-Gal4*, *Or92a-Gal4*, and *Or42b-Gal4* (Leslie Vosshall); *UAS-DTI/CyO* and *UAS-DTI*$_{III}$ (Leslie Stevens). *UAS-CD8:GFP*$_{I}$, *UAS-CD8:GFP*$_{II}$, and *UAS-CD8:GFP*$_{III}$ were obtained from the Bloomington Stock Center. *Or10a*^{f03694} and *Or42a*^{f04305} are indexed on Flybase as pBac insertions and were obtained from Bloomington. We found that the *Or42a*^{f04305} stock had a second mutation that specifically affects the pb2A and pb3B neurons (Figures S5 and S6). This mutation is on the third chromosome and most likely affects the odorant receptor genes *Or85e* and *Or85d*, which are expressed in the pb2A and pb3B neurons, respectively. We term this mutation Δ*85*. The *Or42a*^{f04305} and Δ*85* mutations were separated using standard genetic crosses. The genotypes used in all experiments are listed in Table S1.

ORN Recordings

Flies were immobilized in the trimmed end of a plastic pipette tip. A reference electrode filled with *Drosophila* saline was inserted into the eye, and a sharp saline-filled glass capillary (tip diameter < 1μm) was inserted into a sensillum. Sensilla were visualized using an Olympus BX51WI microscope with a 50× air objective. Sensillum types were identified based on their morphology and their characteristic responses to a panel of odors (de Bruyne et al., 1999, 2001). For recordings from flies with rescued VA7l ORNs, we recorded semirandomly from all three types of sensilla on the maxillary palp (pb2 sensilla which contain the VA7l ORNs are slightly thinner than pb1 and pb3, which allowed us to bias our recordings toward pb2). Voltage signals were acquired with an A-M Systems Model 2400 amplifier (10MΩ headstage). Signals were low-pass filtered at 2 kHz and digitized at 10 kHz. ORN spikes were detected off-line using routines in IgorPro (Wavemetrics). In all cases except ab1 sensilla, spikes could be easily sorted based on their different shapes. In the case of ab1 sensilla, there are four neurons and hence four kinds of spikes, of which the DL1 ORN spikes are the smallest. To get accurate estimates for the response of the DL1 ORNs to some odors, we needed to kill other neurons in this sensillum (see Table S1). Due to genetic constraints, this was not done for the mutant DL1 ORNs. Hence, responses to some odors that activate the other neurons in this sensillum strongly could not be determined, and are marked (‡) in Figure S1. Local field potentials were recorded with an electrode inserted into the antenna or maxillary palp and a reference electrode in the eye.

PN Recordings

Whole-cell recordings from PNs were performed in vivo as previously described (Wilson and Laurent, 2005). For some experiments, the antennal nerves were severed with fine forceps just prior to recording. The composition of the internal patch-pipette solution was as follows: 140 mM potassium aspartate, 10 mM HEPES, 4 mM MgATP, 0.5 mM Na_3GTP, 1 mM EGTA, 1 mM KCl, 13 mM biocytin hydrazide (pH = 7.3; osmolarity adjusted to ~265 mOsm). The composition of the external saline solution was as follows: 103 mM NaCl, 5 mM *N*-tris(hydroxymethyl) methyl-2-aminoethane-sulfonic acid, 8 mM trehalose, 10 mM glucose, 26 mM $NaHCO_3$, 1 mM NaH_2PO_4, $CaCl_2$, and 1.5 mM $MgCl_2$. Osmolarity was adjusted to 270–275 mOsm. The saline was bubbled with 95% O_2/5% CO_2 and reached a final pH = 7.3. Voltage recordings were obtained with an A-M Systems Model 2400 amplifier in the current clamp mode (10 MΩ headstage). Signals were low-pass filtered at 5 kHz and digitized at 10 kHz. An Olympus BX51WI microscope with a 40× water-immersion objective, IR-DIC optics, and a fluorescence attachment was used to obtain recordings under visual control. One neuron was recorded per brain, and the morphology of each cell was visualized post hoc with biocytin histochemistry. Histochemistry with biocytin-streptavidin and nc82 antibody was performed as described previously (Wilson and Laurent, 2005), except that in the secondary incubation we used 1:250 goat anti-mouse:AlexaFluor 633 and 1:1000 streptavidin:AlexaFluor 568 (Molecular Probes). The nc82 antibody (used to outline glomerular boundaries) was obtained from the Developmental Studies Hybridoma Bank (University of Iowa). Histochemistry with α-CD8 antibody (Figures 1B, 5C, and S1A) was performed as described previously (Wilson and Laurent, 2005). Glomeruli were identified using published maps (Laissue et al., 1999; Couto et al., 2005).

Olfactory Stimulation

Odors were diluted in paraffin oil at a ratio of 1:100 (except for the VM7-only experiments, see below). Odors in Figure 4 are benzaldehyde (BNZ), butyric acid (BUA), 2,3-butanedione (BUD), 1-butanol (BUT), cyclohexanone (CYH), cis-3-hexen-1-ol (CIS), ethyl butyrate (EBA), ethyl acetate (ETA), geranyl acetate (GER), methyl salicylate (MSL), 3-methylthio-1-propanol (MTP), 4-methyl phenol (MPH), γ-valerolactone (VAL). Odors used for stimulation of rescued VA7l ORNs (Figures 6A and 6C, 8A–8C, and 9) were 4-methyl phenol, benzaldehyde, methyl salicylate, ethyl acetate, 1-butanol, cyclohexanone, 3-octanol, and paraffin oil. For selective stimulation of VM7 ORNs (Figures 5E, 6B, 6D, 7A, and 8D–8F), dilution ratios in paraffin oil were adjusted for most odors to achieve specific stimulation; odors were acetone (10^{-4} dilution), 2-butanone (10^{-5}), ethyl acetate (10^{-4}), geranyl acetate (10^{-3}), hexanal (10^{-4}), hexyl acetate (10^{-4}), isoamyl acetate (10^{-6}), methyl acetate (10^{-4}), octanal (10^{-4}), propanal (10^{-4}), 2-pentanone (10^{-4}), trans-2-hexenal (10^{-4}), butyric acid (10^{-2}), and paraffin oil. Odor-source details are at http://wilson.med.harvard.edu/odors.html. Odors were delivered with a custom-built olfactometer. A continuous stream of charcoal-filtered air (2.2 l/min) was directed over the fly. Switching of a three-way solenoid redirected 200 ml/min of this air through an odor vial, which rejoined the air stream 12 cm from the end of the odor tube. Thus, all odors were diluted 10-fold in air just before reaching the fly. All odor stimuli were applied for 500 ms. The odor tube was ~8 mm in diameter and terminated ~8 mm from the fly.

Data Analysis

Data were analyzed using custom software written in Igor Pro (Wavemetrics). In Figures 1, 6, 7, and 8, PN voltage traces were averaged over six repeated presentations of each odor and low-pass filtered off-line at 13 Hz to remove spikes before averaging across experiments. Depolarization area was computed as the area under the baseline-zeroed membrane potential over a 500 ms window starting 100 ms after opening of the odor valve. Traces are presented as the mean ± SEM across experiments. Tuning curves in Figure 4 were generated by computing mean firing rate over the 500 ms odor presentation, minus the baseline firing rate.

Supplemental Data

The Supplemental Data for this article can be found online at http://www.neuron.org/cgi/content/full/54/1/89/DC1/.

ACKNOWLEDGMENTS

We thank Barry Dickson, Kei Ito, Liqun Luo, Leslie Vosshall, and Leslie Stevens for gifts of fly stocks. We are grateful to Wade Regehr and members of the Wilson lab for helpful conversations and comments on the manuscript. This work was funded by a grant from the National Institutes of Health (1R01DC008174-01), a Pew Scholars Award, a Smith Family Foundation New Investigators Award, an Armenise-Harvard Junior Faculty Award, and a Loreen Arbus Scholarship in Neuroscience (to R.I.W.). S.R.O is supported by a Predoctoral Fellowship from the National Science Foundation.

Received: January 3, 2007
Revised: March 13, 2007
Accepted: March 15, 2007
Published: April 4, 2007

REFERENCES

Aungst, J.L., Heyward, P.M., Puche, A.C., Karnup, S.V., Hayar, A., Szabo, G., and Shipley, M.T. (2003). Centre-surround inhibition among olfactory bulb glomeruli. Nature *426*, 623–629.

Benton, R., Sachse, S., Michnick, S.W., and Vosshall, L.B. (2006). Atypical membrane topology and heteromeric function of Drosophila odorant receptors in vivo. PLoS Biol. *4*, e20. 10.1371/journal.pbio.0040020.

Berdnik, D., Chihara, T., Couto, A., and Luo, L. (2006). Wiring stability of the adult Drosophila olfactory circuit after lesion. J. Neurosci. *26*, 3367–3376.

Buck, L.B. (1996). Information coding in the vertebrate olfactory system. Annu. Rev. Neurosci. *19*, 517–544.

Christensen, T.A., Waldrop, B.R., and Hildebrand, J.G. (1998). Multitasking in the olfactory system: context-dependent responses to odors reveal dual GABA-regulated coding mechanisms in single olfactory projection neurons. J. Neurosci. *18*, 5999–6008.

Couto, A., Alenius, M., and Dickson, B.J. (2005). Molecular, anatomical, and functional organization of the *Drosophila* olfactory system. Curr. Biol. *15*, 1535–1547.

de Bruyne, M., Clyne, P.J., and Carlson, J.R. (1999). Odor coding in a model olfactory organ: the Drosophila maxillary palp. J. Neurosci. *19*, 4520–4532.

de Bruyne, M., Foster, K., and Carlson, J.R. (2001). Odor coding in the *Drosophila* antenna. Neuron *30*, 537–552.

Dobritsa, A.A., van der Goes van Naters, W., Warr, C.G., Steinbrecht, R.A., and Carlson, J.R. (2003). Integrating the molecular and cellular basis of odor coding in the *Drosophila* antenna. Neuron *37*, 827–841.

Elmore, T., Ignell, R., Carlson, J.R., and Smith, D.P. (2003). Targeted mutation of a Drosophila odor receptor defines receptor requirement in a novel class of sensillum. J. Neurosci. *23*, 9906–9912.

Ennis, M., Zhou, F.M., Ciombor, K.J., Aroniadou-Anderjaska, V., Hayar, A., Borrelli, E., Zimmer, L.A., Margolis, F., and Shipley, M.T. (2001). Dopamine D2 receptor-mediated presynaptic inhibition of olfactory nerve terminals. J. Neurophysiol. *86*, 2986–2997.

Ernst, K.D., and Boeckh, J. (1983). A neuroanatomical study on the organization of the central antennal pathways in insects. III. Neuroanatomical characterization of physiologically defined response types of deutocerebral neurons in Periplaneta americana. Cell Tissue Res. *229*, 1–22.

Fishilevich, E., and Vosshall, L.B. (2005). Genetic and functional subdivision of the *Drosophila* antennal lobe. Curr. Biol. *15*, 1548–1553.

Goldman, A.L., van der Goes van Naters, W., Lessing, D., Warr, C.G., and Carlson, J.R. (2005). Coexpression of two functional odor receptors in one neuron. Neuron *45*, 661–666.

Hallem, E.A., and Carlson, J.R. (2006). Coding of odors by a receptor repertoire. Cell *125*, 143–160.

Hallem, E.A., Ho, M.G., and Carlson, J.R. (2004). The molecular basis of odor coding in the *Drosophila* antenna. Cell *117*, 965–979.

Hayar, A., Karnup, S., Ennis, M., and Shipley, M.T. (2004). External tufted cells: a major excitatory element that coordinates glomerular activity. J. Neurosci. *24*, 6676–6685.

Hoskins, S.G., Homberg, U., Kingan, T.G., Christensen, T.A., and Hildebrand, J.G. (1986). Immunocytochemistry of GABA in the antennal lobes of the sphinx moth Manduca sexta. Cell Tissue Res. *244*, 243–252.

Isaacson, J.S., and Strowbridge, B.W. (1998). Olfactory reciprocal synapses: Dendritic signaling in the CNS. Neuron *20*, 749–761.

Jahr, C.E., and Nicoll, R.A. (1980). Dendrodendritic inhibition: demonstration with intracellular recording. Science *207*, 1473–1475.

Laissue, P.P., Reiter, C., Hiesinger, P.R., Halter, S., Fischbach, K.F., and Stocker, R.F. (1999). Three-dimensional reconstruction of the antennal lobe in Drosophila melanogaster. J. Comp. Neurol. *405*, 543–552.

Larsson, M.C., Domingos, A.I., Jones, W.D., Chiappe, M.E., Amrein, H., and Vosshall, L.B. (2004). Or83b encodes a broadly expressed odorant receptor essential for *Drosophila* olfaction. Neuron *43*, 703–714.

Laurent, G. (2002). Olfactory network dynamics and the coding of multidimensional signals. Nat. Rev. Neurosci. *3*, 884–895.

Leitch, B., and Laurent, G. (1996). GABAergic synapses in the antennal lobe and mushroom body of the locust olfactory system. J. Comp. Neurol. *372*, 487–514.

MacLeod, K., and Laurent, G. (1996). Distinct mechanisms for synchronization and temporal patterning of odor-encoding neural assemblies. Science *274*, 976–979.

Malun, D. (1991). Synaptic relationships between GABA-immunoreactive neurons and an identified uniglomerular projection neuron in the antennal lobe of Periplaneta americana: a double-labeling electron microscopic study. Histochemistry *96*, 197–207.

McGann, J.P., Pirez, N., Gainey, M.A., Muratore, C., Elias, A.S., and Wachowiak, M. (2005). Odorant representations are modulated by intra- but not interglomerular presynaptic inhibition of olfactory sensory neurons. Neuron *48*, 1039–1053.

Mori, K., Nagao, H., and Yoshihara, Y. (1999). The olfactory bulb: coding and processing of odor molecule information. Science *286*, 711–715.

Murphy, G.J., Darcy, D.P., and Isaacson, J.S. (2005). Intraglomerular inhibition: signaling mechanisms of an olfactory microcircuit. Nat. Neurosci. *8*, 354–364.

Ng, M., Roorda, R.D., Lima, S.Q., Zemelman, B.V., Morcillo, P., and Miesenbock, G. (2002). Transmission of olfactory information between three populations of neurons in the antennal lobe of the fly. Neuron *36*, 463–474.

Python, F., and Stocker, R.F. (2002). Immunoreactivity against choline acetyltransferase, gamma-aminobutyric acid, histamine, octopamine, and serotonin in the larval chemosensory system of Drosophila melanogaster. J. Comp. Neurol. *453*, 157–167.

Shang, Y., Claridge-Chang, A., Sjulson, L., Pypaert, M., and Miesenbock, G. (2007). Excitatory local circuits and their implications for olfactory processing in the fly antennal lobe. Cell *128*, 601–612.

Stocker, R.F., Heimbeck, G., Gendre, N., and de Belle, J.S. (1997). Neuroblast ablation in Drosophila P[GAL4] lines reveals origins of olfactory interneurons. J. Neurobiol. *32*, 443–456.

Tanaka, N.K., Awasaki, T., Shimada, T., and Ito, K. (2004). Integration of chemosensory pathways in the *Drosophila* second-order olfactory centers. Curr. Biol. *14*, 449–457.

Thibault, S.T., Singer, M.A., Miyazaki, W.Y., Milash, B., Dompe, N.A., Singh, C.M., Buchholz, R., Demsky, M., Fawcett, R., Francis-Lang,

H.L., et al. (2004). A complementary transposon tool kit for Drosophila melanogaster using P and piggyBac. Nat. Genet. *36*, 283–287.

Urban, N.N., and Sakmann, B. (2002). Reciprocal intraglomerular excitation and intra- and interglomerular lateral inhibition between mouse olfactory bulb mitral cells. J. Physiol. *542*, 355–367.

Wachowiak, M., Cohen, L.B., and Ache, B.W. (2002). Presynaptic inhibition of olfactory receptor neurons in crustaceans. Microsc. Res. Tech. *58*, 365–375.

Wachowiak, M., McGann, J.P., Heyward, P.M., Shao, Z., Puche, A.C., and Shipley, M.T. (2005). Inhibition of olfactory receptor neuron input to olfactory bulb glomeruli mediated by suppression of presynaptic calcium influx. J. Neurophysiol. *94*, 2700–2712.

Wang, J.W., Wong, A.M., Flores, J., Vosshall, L.B., and Axel, R. (2003). Two-photon calcium imaging reveals an odor-evoked map of activity in the fly brain. Cell *112*, 271–282.

Wilson, R.I., and Laurent, G. (2005). Role of GABAergic inhibition in shaping odor-evoked spatiotemporal patterns in the Drosophila antennal lobe. J. Neurosci. *25*, 9069–9079.

Wilson, R.I., Turner, G.C., and Laurent, G. (2004). Transformation of olfactory representations in the Drosophila antennal lobe. Science *303*, 366–370.

Wong, A.M., Wang, J.W., and Axel, R. (2002). Spatial representation of the glomerular map in the *Drosophila* protocerebrum. Cell *109*, 229–241.